Quantum chemical study of the initial surface reactions in atomic layer deposition of TiN on the SiO_2 surface

2006 J. Phys.: Condens. Matter 18 5937

(http://iopscience.iop.org/0953-8984/18/26/013)

INSTITUTE OF PHYSICS PUBLISHING JOURNAL OF PHYSICS: CONDENSED MATTER

J. Phys.: Condens. Matter **18** (2006) 5937–5944 doi:10.1088/0953-8984/18/26/013

Quantum chemical study of the initial surface reactions in atomic layer deposition of TiN on the SiO_2 surface

Hong-Liang Lu, Wei Chen, Shi-Jin Ding, Min Xu, David Wei Zhang[1] and Li-Kang Wang

State Key Laboratory of ASIC and System, Department of Microelectronics, Fudan University, Shanghai 200433, People's Republic of China

E-mail: dwzhang@fudan.edu.cn and dwzhang@fudan.ac.cn

Received 15 January 2006
Published 16 June 2006
Online at stacks.iop.org/JPhysCM/18/5937

Abstract

Cluster calculations employing hybrid density functional theory have been carried out to examine the initial surface reactions in atomic layer deposition (ALD) of TiN thin films on the SiO_2 surface using $TiCl_4$ and NH_3 as precursors. The potential energy surface (PES) of both half-reactions at different temperatures is presented. The first half-reaction between $TiCl_4$ with the SiO_2 surface is activated with an activation barrier of 0.78 eV and an exothermicity of 0.38 eV, suggesting that it is thermodynamically favourable. Also, the NH_3 half-reaction begins with the formation of amido complexes by the replacement of Cl atoms by NH_2, which is endothermic by 0.58 eV with a physisorbed HCl state (HCl-PS1). Formation of the amido complexes can be followed by an elimination reaction to form imido complexes, which has a relatively high activation barrier of 2.51 eV. In addition, the effect of the reaction temperature on the Cl impurity concentrations and film growth rate in the ALD process is also discussed.

1. Introduction

In the past few years, copper (Cu) has been widely used as interconnect metallization for advanced ultra-large-scale integration (ULSI) circuits due to its lower electrical resistivity and higher resistance to electromigration compared with aluminium [1–3]. Despite its superior electrical characteristics, the application of Cu as an interconnect material requires a diffusion barrier in order to prevent Cu migration from entering SiO_2 or other dielectrics [4, 5]. The most widely used deposition technique for the diffusion barriers in modern semiconductor devices has been physical vapour deposition (PVD) and chemical vapour deposition (CVD) [6, 7]. Nevertheless, their inherent disadvantages make them unsuitable for growing conformal barriers on high-aspect-ratio vias and trenches in microelectronic devices with a smaller feature

[1] Author to whom any correspondence should be addressed.

size in the future. Therefore, a new deposition technique needs to be introduced for the continued scaling of semiconductor devices.

Atomic layer deposition (ALD) is expected to be a promising technique for growing conformal thin films on high-aspect-ratio structures [8, 9]. Despite many similarities, clear differences can be found between ALD and CVD. The ALD method is a nonequilibrium process, as the gas flow during the exposure and purge phases of the reaction cycle enables reaction byproducts to be removed from the reactor. The self-limiting nature of ALD facilitates the growth of uniform and conformal thin films with accurate thickness over large areas [10–12]. This means that the method will not build up thickness at the entrance of the bottoms and sidewalls of vias and trenches.

Titanium nitride (TiN) is considered to be one of the favourable materials for barrier metal in Cu interconnection technology because of its thermal stability, good diffusion barrier properties and low electrical resistivity [13–15]. There have been many studies on the ALD of TiN barriers on the SiO_2 surface using $TiCl_4$ and NH_3 as precursors [12, 16–18]. In addition, the ALD of TiN as a metal gate has also been investigated to solve problems such as the gate depletion and dopant penetration for the further scaling of metal oxide semiconductor field effect transistor (MOSFET) devices [19–21]. Experimental data have shown that resistivity with the ALD of TiN appears to be partially correlated to chlorine (Cl) concentration, which decreases with the growth temperature [22]. This implies that the Cl impurity concentrations decrease at elevated temperatures. On the other hand, with increasing temperature, a decreasing growth rate per cycle is also observed [18].

The kinetics of TiN CVD surface reactions using $TiCl_4$ and ammonia as precursors have been calculated previously [23–25]. However, the detailed reaction mechanism of TiN ALD on the SiO_2 surface is not fully understood. It is also well known that initial film growth onto substrates is inhibited in many ALD process. Hence, the fundamental growth mechanism of TiN ALD on the SiO_2 surface is of primary interest and importance in order to find the best conditions for obtaining high-quality films. In the present work, first-principles calculations based on hybrid density functional theory (DFT) are carried out to investigate the initial surface reactions of TiN ALD on the SiO_2 surface using $TiCl_4$ and NH_3 as precursors to elucidate the film growth mechanism.

2. Calculation method

To investigate the possible reaction pathways of TiN ALD on the SiO_2 surface, a $(SiH_3O)_3Si$–OH cluster is chosen to represent the SiO_2–OH, in which the central silicon atom is terminated by an –OH group and combines with all three oxygen atoms bonding to the silicon atoms terminated by three hydrogen atoms. The geometries and single-point energies of the reactants, intermediate state, transition state, and products of the reaction are optimized. The reaction pathways are constructed by a potential energy surface (PES) scan. All of the calculations presented in this work are carried out using the Gaussian 03 quantum chemistry program [26]. The results described here are obtained using the B3LYP hybrid density functional, which corresponds to Becke's three-parameter exchange functional (B3) along with the Lee–Yang–Parr gradient-corrected correlation functional (LYP) [27]. The electronic wavefunction is expanded by using Gaussian basis sets. All of the atoms are described using the 6–31G(d) basis set. The optimizations are performed by finding stationary points followed by frequency calculations needed to verify the nature of the stationary points on the PES, including energy minima (all positive frequencies) and transition states (one imaginary frequency). The clusters are fully relaxed without any constraints. Energies reported here include zero-point energy corrections.

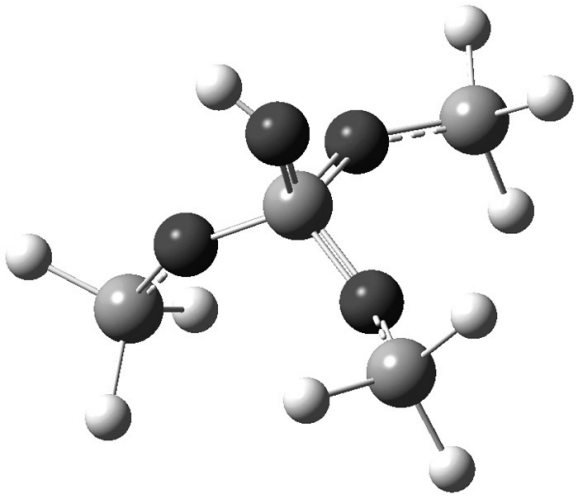

Figure 1. $(SiH_3O)_3Si$–OH cluster model representing SiO_2–OH^* surface. The black, small grey, and white balls represent O, Si, and H atoms, respectively.

To ensure the accuracy of the computed reaction energies, larger basis sets have also been used to calculate the single-point energies of optimized critical points. We extended the basis set to the B3LYP/6-311G(d) and B3LYP/6 − 311++G(3df, 2p) level of theory on both half-reactions. Both approaches resulted in similar energies, as found using B3LYP/6-31G(d), the average differences in relative energies were less than ±0.09 eV.

3. Results and discussion

The optimized geometry of the $(SiH_3O)_3Si$–OH cluster is shown in figure 1. The initial surface reactions of TiN ALD between the precursors and the SiO_2 surface can be separated into two half-reactions. In the first half-reaction, $TiCl_4$ reacts with an SiO_2 surface –OH group, liberating HCl and forming a SiO_2–O–$TiCl^*$ terminated surface, where the asterisks denote the active surface species. Following an inert gas (e.g. N_2) purging period, NH_3 is pulsed into the reactor and reacts with –$TiCl^*$ groups, forming –$TiNH_2^*$ during the second half-reaction.

The optimized geometries of the total system along the two half-reactions are shown in figure 2. The PES along with the Gibbs free energies at different temperatures of the first half-reaction, which represents the reaction of gaseous $TiCl_4$ on the SiO_2–OH^* surface, are shown in figure 3. The corresponding numerical values of reaction energies at 0 K and Gibbs free energies at 298, 450 and 600 K are listed in table 1. When $TiCl_4$ approaches the SiO_2 surface, it forms a $TiCl_4$ chemisorbed state ($TiCl_4$-CS) through the interaction between an empty d-orbital of a Ti atom and the oxygen lone-pair electrons. The electron donation from an oxygen lone-pair to a Ti atom weakens the Ti–Cl bonds. This can be seen from the change in Ti–Cl bond lengths. The Ti–Cl bonds increase from 2.180 Å in $TiCl_4$ to 2.241 and 2.205 Å in the $TiCl_4$-CS. Then the Cl atom of the longer Ti–Cl bond reacts with one hydrogen atom from the surface –OH group by a transition state ($TiCl_4$–TS) to form the byproduct (HCl). The $TiCl_4$–TS structure has Ti–Cl and O–H bond lengths of 2.748 and 1.251 Å, which are elongated by 23% and 29% with respect to the $TiCl_4$-CS. HCl can desorb from the surface to reach an HCl desorption state (HCl-DS1) spontaneously. At last, the surface functional group transforms from a SiO_2–OH^* surface to a SiO_2–O–$TiCl_3^*$ surface. As can be seen from figure 3, when

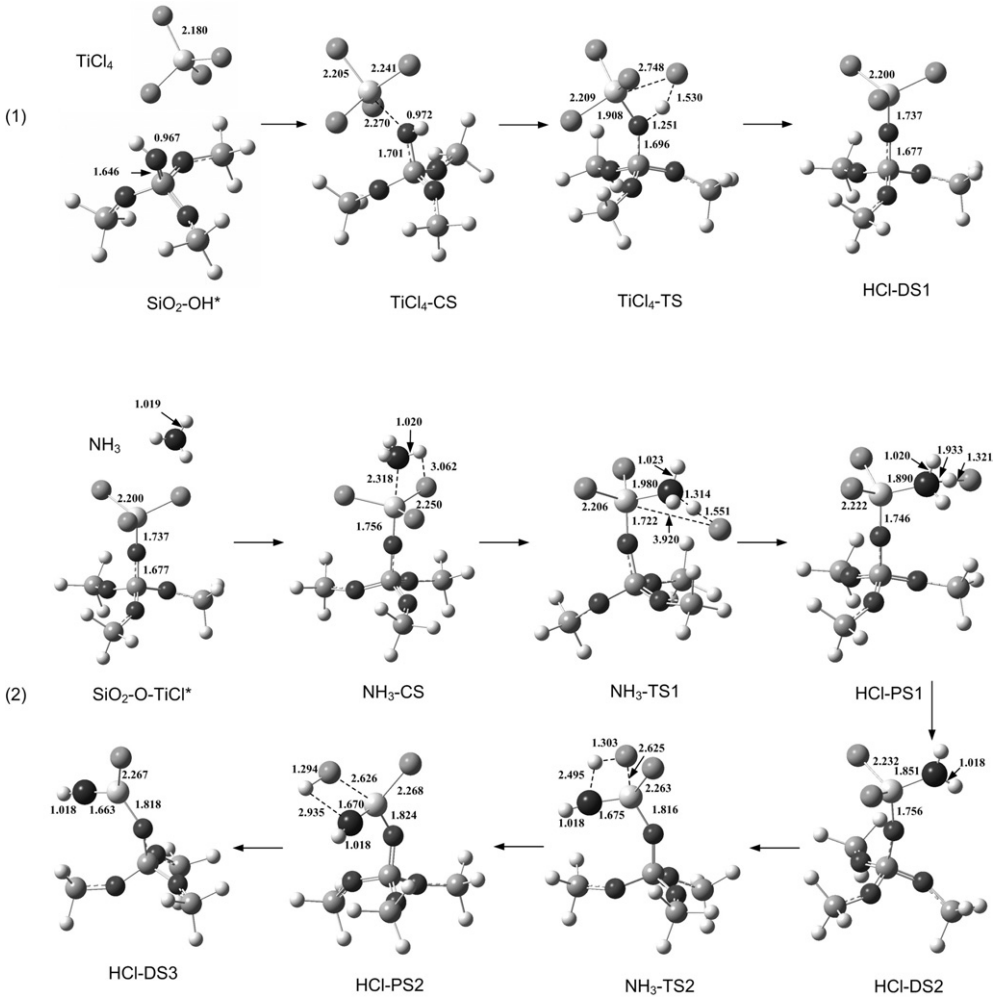

Figure 2. The optimized geometries of the total system along the two half-reactions: (1) the first half-reaction; (2) the second half-reaction. The bond lengths are shown in Å. The small black, big black, light grey, small white, dark grey, and big white balls represent O, N, Si, H, Cl, and Ti atoms, respectively.

$TiCl_4$ adsorbs as molecules on a SiO_2–OH^* surface site, the adsorption energy is 0.46 eV. Also, a high activation barrier of 0.78 eV is needed for the reaction. It is obvious that this reaction is exothermic by 0.38 eV. This is in agreement with the calculation results of Tanaka *et al*, where SiOH clusters are used to represent the SiO_2–OH^* surface sites [25].

The second half-reaction involves the reaction of ammonia with surface chlorine groups. This is the formation of amido complexes SiO_2–O–$TiCl_x(NH_2)^*_{3-x}$ by ligand exchange reactions and of imido complexes by subsequent elimination reactions, where x has values of 0–2. The reaction pathway for the replacement of the first Cl atom bonded to Ti by NH_2 is shown in figure 4. In addition, the corresponding numerical values of reaction energies at 0 K and Gibbs free energies at 298, 450 and 600 K for this half-reaction are summarized in table 2. The first step of this half-reaction involves the adsorption of NH_3 onto the SiO_2–O–$TiCl^*_3$ surface to form a chemisorbed ammonia complex (NH_3-CS). Our calculation results

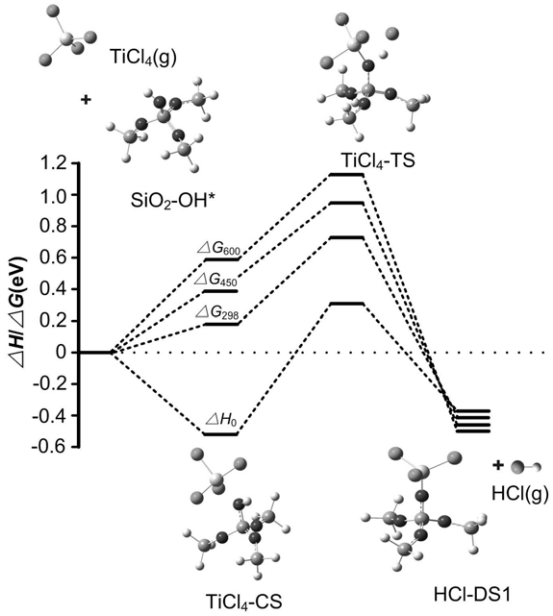

Figure 3. Reaction pathway for the reaction of gaseous $TiCl_4$ on SiO_2–OH* surface. The black, light grey, small white, dark grey, and big white balls represent O, Si, H, Cl, and Ti atoms, respectively.

Table 1. Reaction energies at 0 K (ΔH_0) and Gibbs free energies (ΔG) at 298, 450 and 600 K for SiO_2–OH^* + $TiCl_4$ half-reaction. All energies are shown in eV.

	$TiCl_4$-CS	$TiCl_4$-TS	HCl-DS1
ΔH_0	−0.46	0.32	−0.38
ΔG_{298}	0.18	0.74	−0.41
ΔG_{450}	0.39	0.95	−0.46
ΔG_{600}	0.59	1.14	−0.50

Table 2. Reaction energies at 0 K (ΔH_0) and Gibbs free energies (ΔG) at 298, 450 and 600 K for SiO_2–O–$TiCl_x^*$ + NH_3 half-reaction. All energies are shown in eV.

	NH_3-CS	NH_3-TS1	HCl-PS1	HCl-DS2	NH_3-TS2	HCl-PS2	HCl-DS3
ΔH_0	−0.70	0.58	0.49	0.58	3.09	3.10	3.62
ΔG_{298}	−0.29	1.09	0.95	0.58	3.14	3.18	3.31
ΔG_{450}	−0.07	1.38	1.20	0.49	3.16	3.20	3.26
ΔG_{600}	0.15	1.65	1.45	0.56	3.23	3.23	2.99

show that the adsorption energy is 0.70 eV. This stable complex is formed where the interaction between an empty d-orbital of a Ti atom and the nitrogen lone-pair electrons occurs. The weakening Ti–Cl bond also increases from 2.200 Å in the HCl-DS1 to 2.250 Å in this complex. The physisorbed HCl complex (HCl-PS1) is then formed through the reaction of a hydrogen atom from the incoming ammonia and a Cl atom from the SiO_2–O–$TiCl_3^*$ surface. The energy of the transition state (NH_3–TS1) leading to the formation of the HCl-PS1 is 1.28 eV and the reaction is endothermic by 1.19 eV relative to the NH_3-CS. Finally, HCl desorbed to reach its

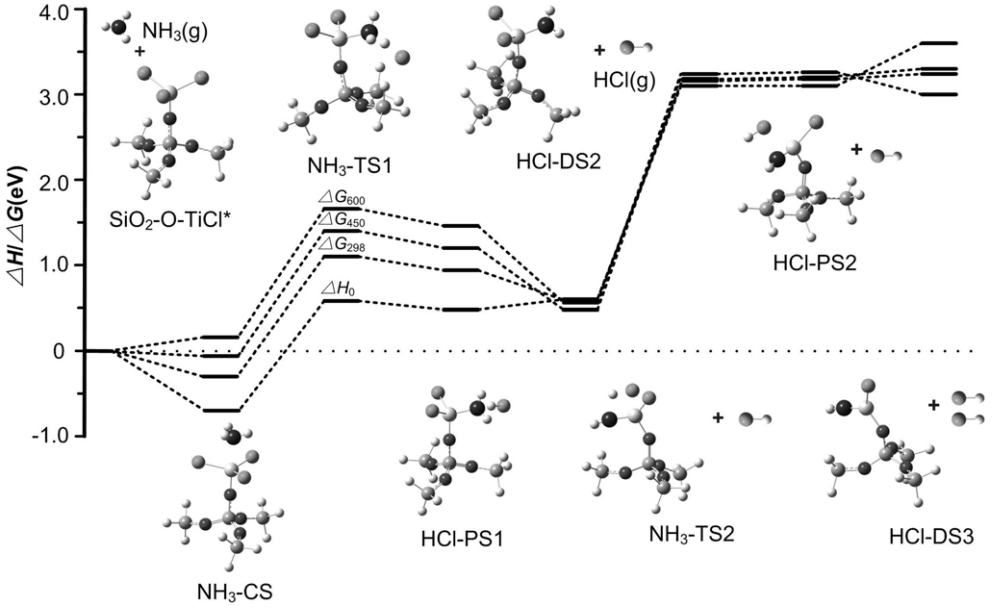

Figure 4. Reaction pathway for the reaction of NH_3 on SiO_2–O–TiCl* surface. The small black, big black, light grey, small white, dark grey, and big white balls represent O, N, Si, H, Cl and Ti atoms, respectively.

desorption state (HCl-DS2) with an energy of 0.09 eV relative to the HCl-PS1. During the process NH_3-CS → NH_3-TS1 → HCl-PS1, the Ti–N and H–Cl bonds change from 2.318 and 3.062 Åto 1.980 and 1.551 Åand to 1.890 and 1.321 Å, respectively. All of them indicate the formation of a Ti–N bond and the byproduct (HCl). Cross *et al* [23] and Siodmiak *et al* [24] found similar reaction pathways in their *ab initio* theoretical studies of TiN CVD. However, their activation barriers are higher, which may be the effect of the SiO_2 substrate or basis sets used in the present work. Further ammonia exposure will result in replacement of the second and third Cl atoms from the SiO_2–O–Ti$(NH_2)_{3-x}$–Cl_x^* ($x = 1$ or 2) sites, which proceeds through an analogous mechanism. The reactions are endothermic by 0.58, 0.79 and 0.94 eV for the first, second and third Cl removals, respectively. This suggests that the process becomes more difficult as more chlorines are replaced by NH_2.

In addition, formation of the amido complexes can be followed by the elimination of HCl, which results in imido complexes [23]. The calculated reaction mechanism is also shown in figure 4. The Ti–N bond over the course of the elimination reaction shows a value of 1.851 Å in the HCl-DS2, shortening to 1.675 Å in the transition state (NH_3-TS2) and 1.670 Å in the HCl physisorbed state (HCl-PS2), and finally becoming 1.663 Å in the HCl desorption state (HCl-DS3). As seen in table 2, the formation of an imido complex has an activation barrier of 2.51 eV and is endothermic by 3.04 eV relative to HCl-DS2, suggesting that the reaction is not thermodynamically and kinetically favourable. Cross *et al* studied the reaction forming imido complexes, and found similar energetics for HCl elimination along the reaction path [23].

As can be seen from figures 3 and 4, both the $TiCl_4$-CS and the NH_3-CS have lower energies than the dissociated products. As a result, the probability of adsorbing molecules being trapped in the molecularly adsorbed state is higher than that of dissociating. This trapped effect will hinder the reaction's progress, as the dissociated products are desired because they are necessary to continue the next half-reaction cycle in ALD. Moreover, it will result in the

incorporation of Cl atoms in the film. It is well known that Cl contamination will cause reliability problems in device performance. However, the free energies of the adsorbed complex and transition state increase relative to the reactant and product free energies with increasing temperature, as shown in tables 1 and 2. This is mainly due to an entropic effect [28, 29]. As a result, the stability of the adsorbed complexes can then be reduced by increasing temperature, which will result in the decrease of Cl impurity concentration in the grown film. This result has been observed by Elers *et al*, who found that the chlorine concentration was inversely proportional to the deposition temperature [12]. In addition, physisorbed byproducts (HCl) can easily desorb from the surface at elevated temperatures rather than readsorbing and blocking surface sites from further adsorption of the precursor, which leads to slower growth rates. The desorbed HCl is then purged out of the reactor by the inert gas, which drives the reaction towards the products under a nonequilibrium ALD process.

Nevertheless, the temperature only slightly affects the free energies of the products, because the entropy difference between the reactants and the products is found to be small. Furthermore, the lower desorption barrier will make more chemisorbed precursors desorb from the surface instead of further dissociating to form the film and byproducts. This is in agreement with previous reports of experiments [17, 30]. The growth rate of the initial surface reaction has been observed to decrease at elevated temperatures. As a result, although the population of the trapped complexes decrease with temperature, longer gaseous reactant exposure times are needed to maintain a high gaseous pressure in order to minimize desorption of the adsorbed precursor molecules from the surface. A longer NH_3 pulse time has also been found to increase the film growth rate [17].

4. Conclusion

In conclusion, we have investigated the initial reaction mechanism of TiN ALD on the SiO_2 surface using $TiCl_4$ and NH_3 gaseous precursors. The resulting changes in reaction energy at 0 K, together with the Gibbs free energies at 298, 450 and 600 K for both half-reactions, are presented. The results reveal that both half-reactions have relatively stable chemisorbed states, with formation energies of 0.46 and 0.70 eV, respectively. The stable chemisorbed complexes not only hinder the reaction progress but also result in the incorporation of Cl atoms in the film. Consequently, a high surface temperature is required to reduce the stability of the trapped complexes in order to drive them towards dissociation and to decrease the Cl concentration. However, the adsorbed precursor molecules prefer to emanate rather than react on the corresponding surfaces at elevated temperatures. As a result, longer precursors exposure times are necessary to maintain a high gaseous pressure to minimize desorption of the adsorbed precursor molecules from the surface.

Acknowledgments

This work is supported by the National Natural Science Foundation of China, the Science and Technology Committee of Shanghai under Grant No. 04JC14013, the Program for New Century Excellent Talents in University (NCET-04-0366), and the Shanghai Pujiang Program (05PJ14017).

References

[1] Tu K N 2003 *J. Appl. Phys.* **94** 5451
[2] Murarka S P 1997 *Mater. Sci. Eng.* R **19** 87

[3] Venkatesan S *et al* 1997 *IEEE Int. Electron Devices Mtg* p 769
[4] Kaloyeros A E and Eisenbraun E 2000 *Annu. Rev. Mater. Sci.* **30** 363
[5] Kim H 2003 *J. Vac. Sci. Technol.* B **21** 2231
[6] Moriyama M, Kawazoe T, Tanaka M and Murakami M 2002 *Thin Solid Films* **416** 136
[7] Fouilland L, Imhoff L, Bouteville A, Benayoun S, Remy J C, Perriere J and Morcrette M 1998 *Surf. Coat. Technol.* **101** 146
[8] Suntola T 1992 *Thin Solid Films* **216** 84
[9] Leskela M and Ritala M 2003 *Angew. Chem. Int. Edn* **42** 5548
[10] Kim J, Hong H, Oh K and Lee C 2003 *Appl. Surf. Sci.* **210** 231
[11] Ritala M, Asikainen T, Leskela M, Jokinen J, Lappalainen R, Utriainen M, Niinisto L and Ristolainien E 1997 *Appl. Surf. Sci.* **120** 199
[12] Elers K-E, Saanila V, Soininen P J, Li W-M, Kostamo J T, Haukka S, Juhanoja J and Besling W F A 2002 *Chem. Vapor Depos.* **8** 149
[13] Kim S-H, Chung D-S, Park K-C, Kim K-B and Min S-H 1999 *J. Electrochem. Soc.* **146** 1455
[14] Lee H J, Sinclair R, Li P and Roberts B 1999 *J. Appl. Phys.* **86** 3096
[15] Mei Y J, Chang T C, Hu J C, Hu J C, Chen L J, Yang Y L, Pan F M, Wu W F, Ting A and Chang C Y 1997 *Thin Solid Films* **308/309** 594
[16] Li S, Dong Z L, Lim B K, Liang M H, Sun C Q, Gao W and Park H S 2002 *J. Phys. Chem.* B **106** 12797
[17] Satta A, Schuhmacher J, Whelan C M, Vandervorst W, Brongersma S H, Beyer G P, Maex K, Vantomme A, Viitanen M M, Brongersma H H and Besling W F A 2002 *J. Appl. Phys.* **92** 7641
[18] Satta A, Vantomme A, Schuhmacher J, Whelan C M, Sutcliffe V and Maex K 2004 *Appl. Phys. Lett.* **84** 4571
[19] Sell B, Sanger A and Krautschneider W 2003 *J. Vac. Sci. Technol.* B **21** 931
[20] Westlinder J, Schram T, Pantisano L, Cartier E, Kerber A, Lujan G S, Olsson J and Groeseneken G 2003 *IEEE Electron. Device Lett.* **24** 550
[21] Park D-G, Lim K-Y, Cho H-J, Cha T-H, Yeo I-S, Roh J-S and Park J W 2002 *Appl. Phys. Lett.* **80** 2514
[22] Kim D H, Kim J J, Park J W and Kim J J 1996 *J. Electrochem. Soc.* **143** L188
[23] Cross J B and Schlegel H B 2000 *Chem. Mater.* **12** 2466
[24] Siodmiak M, Frenking G and Korkin A 2000 *J. Mol. Model.* **6** 413
[25] Tanaka T, Nakajima T and Yamashita K 2002 *Thin Solid Films* **409** 51
[26] Frisch M J *et al* 2003 *Gaussian 03, Revision B. 05* (Pittsburgh, PA: Gaussian)
[27] Becke A D 1993 *J. Chem. Phys.* **98** 1372
[28] Widjaja Y and Musgrave C B 2002 *J. Chem. Phys.* **117** 1931
[29] Heyman A and Musgrave C B 2004 *J. Phys. Chem.* B **108** 5718
[30] Ritala M, Leskela M, Rauhala E and Haussalo P 1995 *J. Electrochem. Soc.* **142** 2731